Analysis of transmission lines considering frequency-dependent parameters with linear and nonlinear loads

Zahra Bouzidi[1], Hicham Rouijaa[2], Abdelaziz El Idrissi [1], and Mohamed Saih[3]*

[1]Laboratory of Electrical Systems, Energy Efficiency and Telecommunications, Faculty of Science and Technology, Cadi Ayyad University, Marrakesh, Morocco
[2]Laboratory of Systems Analysis and Information Processing, Faculty of Science and Technology, HASSAN 1 University, Settat, Morocco
[3]Laboratory of Automatic, Energy Conversion and Microelectronics, Faculty of Science and Technology, SULTAN MOULAY SLIMAN University, Beni Mellal, Morocco

Abstract. The primary objective of this paper is to model transmission lines with frequency-dependent parameters loaded with linear and nonlinear terminations using an approach based on Pade approximations. To validate our algorithm in the case of lines with constant losses and frequency-dependent parameters, examples of applications in the time and frequency domains are presented. The simulations and obtained results are reported and analysed.

1 Introduction

A transmission line is constructed using a conductor and a return (single transmission lines) or several conductors with a return (Multiconductor transmission lines), and its role is to transport energy from one place to another.

The modelling of transmission lines is more complicated than modelling discrete elements since the parameters of a line are distributed and generally dependent on the frequency. The analysis of transmission lines with frequency-dependent parameters is relevant for the design of high-speed applications. The measurements in [1] and [2] show that ignoring the effect of the dependence of the transmission line parameters leads to considerable errors in the simulation results.

The question therefore, is how to model a transmission line to simulate it on a computer. Many researchers have extensively researched This topic, especially since the 1960s, and even today, considerable work has been devoted to the development of precise and fast models (in terms of calculations). Note, for example, the work of Semlyen & Dabuleanu [3], Marti [4] and Marti [5].

Transmission lines have been modelled and analysed using several techniques and models[6].; the traditional lumped circuit segmentation macro-model allows the transmission line to be represented as a circuit model equivalent to the resistance, inductance, capacitance, and conductance RLCG-equivalent circuit model. Typical examples of such circuits are lumped-p or lumped-T circuits, which can be used for either time- or frequency-domain analyses of the line. These circuits can also be used in the analysis of multi--conductor transmission lines (MTL) [6], which complicates the equivalent circuit considerably. The method of characteristics or Branin's method [7], [8] is able to analyse an ideal transmission line by representing it in the form of a quadruple. The advantage of this quadruple form is that it does not presuppose the load conditions applied at its ends; however, this model is limited to only lossless lines.

An original method [9], [10] based on the Padé approximation makes it possible to model transmission lines in the time and frequency domains using the Padé macro-model.

This macro-model is decomposed into a set of first- and second-order cells. The cells that make up the macro-model are represented by admittance matrices. The number of these cells depends on the order of the Pade approximation of the matrix exponential, solution of the telegrapher's equation.

The aim of this paper is to integrate frequency-dependent parameters into the Padé approximation macro-model.

The paper is organised as follows. In Section 2, the fundamental aspects of the Pade approximation method are reviewed. Section 3 provides a numerical example to illustrate the validity of the Pade approximation macro-model and its application to a variety of interconnected structures.

2 Transmission lines with frequency-dependent parameters

When the frequency increases, an electric field is created, which causes the current distribution of conduction to change. As the frequency increases, the

* Corresponding author: zahra.bouzidi@edu.uca.ma

resistance and inductance per unit length change. These changes are divided into two categories: the effect of proximity and the effect of the skin. Due to the skin effect, the conductor is subjected to a variable frequency current with no applied external magnetic field due to the penetration of the internal magnetic field. In contrast to the skin effect, which is unique to a single conductor, the proximity effect occurs when multiple conductors are sufficiently close together.

2.1 Modelling of transmission line parameters

For simplicity of presentation, the discussion will concentrate on single transmission line structures.
The skin effect of transmission lines has been presented in the circuit configurations shown in Fig.1 [11], [12].

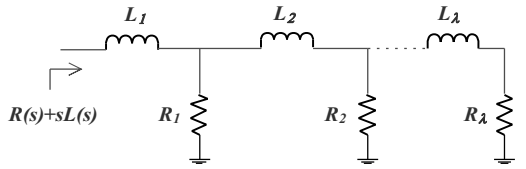

Fig. 1. Circuit configurations to model the frequency-dependency of R(s) + L(s)

Consider the transmission line represented by the following set of telegrapher's equations:

$$\begin{cases} \frac{\partial}{\partial z} V(z,s) = -(R + sL) I(z,s) \\ \frac{\partial}{\partial z} I(z,s) = -(G + sC) V(z,s) \end{cases} \quad (1)$$

Where R, L, C and G are the per unit length parameters (non-negative definite symmetric matrices).
The solution of the system in Eq. (1) can be written in the Laplace domain using the exponential function as follows:

$$\begin{bmatrix} V(l,s) \\ I(l,s) \end{bmatrix} = e^{z} \begin{bmatrix} V(0,s) \\ I(0,s) \end{bmatrix} \quad (2)$$

Where l is the length of the line.

We will use a matrix-rational function to approximate the exponential matrix, as follows:

$$e^{z} = B_{kh}^{-1}(Z) A_{kh}(Z) \quad (3)$$

Where A_{kh} (Z) and B_{kh} (Z) are polynomial matrices written as closed-form Pade rational functions [13] as shown below.

$$B_{kh}(Z) = \sum_{j=0}^{k} \frac{(h+k-j)!\, k!}{(h+k)!\, j!\, (k-j)!} (-Z)^j$$
$$A_{kh}(Z) = \sum_{j=0}^{h} \frac{(h+k-j)!\, h!}{(h+k)!\, j!\, (h-j)!} Z^j \quad (4)$$

The Pade approximation order is represented by k and h.

The product of polynomials $B_{kh}^{-1}(Z) A_{kh}(Z)$ can be represented in terms of poles and zeros using the diagonal Pade approximation (h=k=q).

For even values of q:

$$B_{qq}^{-1}(Z) A_{qq}(Z) = \prod_{i=1}^{q/2} [(u_i I - Z)(u_i^* I - Z)]^{-1} [(u_i I + Z)(u_i^* I + Z)] \quad (5a)$$

For odd values of q:

$$B_{qq}^{-1}(Z) A_{qq}(Z) = (u_0 I - Z)^{-1} (u_0^* I + Z) \prod_{i=1}^{(q-1)/2} [(u_i I - Z)(u_i^* I - Z)]^{-1} [(u_i I + Z)(u_i^* I + Z)] \quad (5b)$$

$u_i = x + j y_i$: Complex pole of polynomial $B_{qq}(Z)$
u_0 : Real pole of polynomial $B_{qq}(Z)$

From the pole-zero pairs represented by Eq. (4) and Eq. (5), the transmission line can be modelled using a Pade macro-model. This macro-model consists of a set of first and second order cells, in which each subsection is composed of predetermined constants u_0 (real-pole), u_i (complex-pole) and the per unit length parameters, whose number depends on the order of the Pade approximation.

$$\begin{bmatrix} V_{i+1} \\ I_{i+1} \end{bmatrix} = \left[B_{qq}^{-1}\right]_i \left[A_{qq}\right]_i \begin{bmatrix} V_i \\ I_i \end{bmatrix} \quad (6)$$

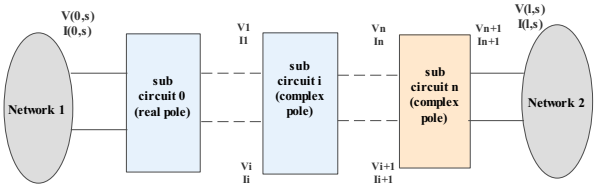

Fig. 2. Equivalent circuit of the line in the sense of Padé: represented by pole-zero section.

Where V(0,s) , I(0,s), V(l,s) and I(l,s) represent the terminal voltages and currents. Vi+1, Ii+1, Vi and Ii represent the internal voltages and currents created by the Pade macro-model.

2.2 Modelling with linear elements

Each subsection in Eq. (6) is converted into the Y-parameter to represent the circuit for transmission lines with frequency-dependent parameters in terms of resistor, inductors, capacitors and ideal transformers.

- Complex pole-zero subsection

$$Y_{11} = Y_{22} = \frac{(x_i^2 + y_i^2)}{4 x_i l} (a(s))^{-1} + \frac{a(s) l}{4 x_i} + x_i (a(s) l + \frac{(x_i^2 + y_i^2)}{l} (b(s))^{-1})^{-1}$$

$$Y_{12} = Y_{21} = \frac{(x_i^2 + y_i^2)}{4 x_i l} (a(s))^{-1} + \frac{b(s) l}{4 x_i} - x_i (a(s) l + \frac{(x_i^2 + y_i^2)}{l} (b(s))^{-1})^{-1}$$

Real pole-zero subsection

$$Y_{11} = Y_{22} = \frac{a_0}{2l} (a(s))^{-1} + \frac{l}{2 a_0} (b(s))$$

$$Y_{12} = Y_{21} = -\frac{a_0}{2l} (a(s))^{-1} + \frac{l}{2 a_0} (b(s))$$

The circuit topologies of the complex pole-zero subsection and the real pole-zero subsection are shown in Fig. 3 and Fig. 4, respectively.

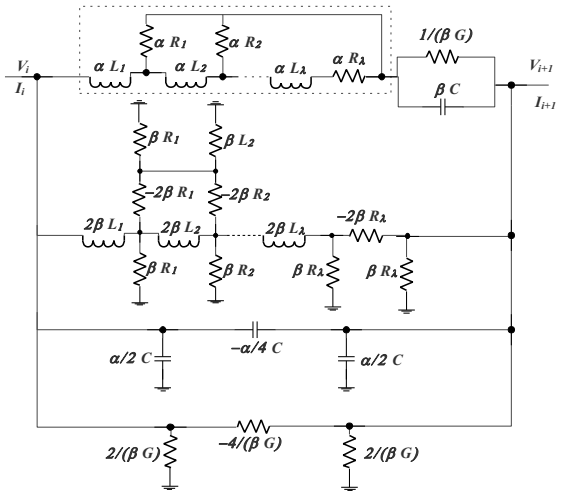

Fig. 3. Circuit topology of the complex pole-zero subsection

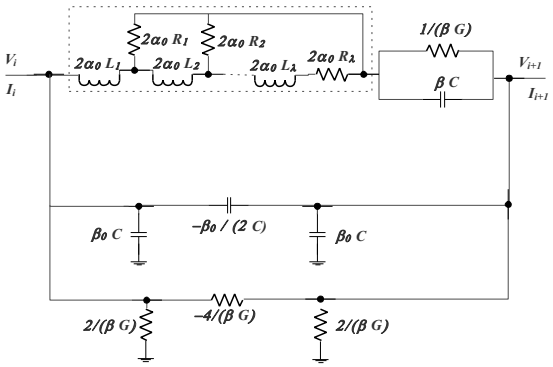

Fig. 4. Circuit topology of the real pole-zero subsection

The Pade approximation macromodel decomposes, as we have already seen, into a set of cells with real poles and with complex poles. The application of the MNA method [14] to each type of cell leads to matrices G and C.

3 Simulation and results

To demonstrate the points raised in the preceding section, we used the example shown in Fig. 5. We compared the simulation results obtained using Pade approximation with the results from the traditional lumped-circuit segmentation macro-model and Branin's method in Emcap2000-Esacap circuit simulator [16]. Pade approximation model is valid in both the time and frequency domains.

We considered a single transmission line of 1cm length see Fig. 5. The in and out charges equalled 50 ohms, as indicated in Fig. 6.

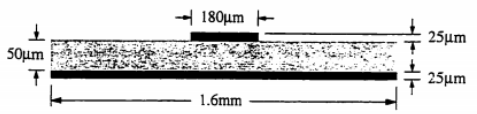

Fig. 5. Conductor over a ground plane.

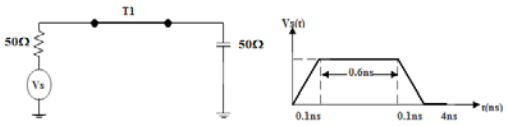

Fig. 6. Electrical representation of the line in Fig.5

3.1 Frequency–independent parameters

We first assumed the line to be lossless and the line parameters to be:

R=50Ω, G=0, C= 90PF et L= 2.65E-7 H.

The circuit in Fig. 6 was analysed in the time and frequency domains using three different approaches: the Branin method, the traditional lumped-circuit segmentation macro-model (decomposed into 100-cascaded cells) and the Pade approximation method (the order of Pade approximation used in this case was 20).

The waveform evolution of the line as a function of time is shown in Fig. 7, and Fig. 8 presents the frequency response.

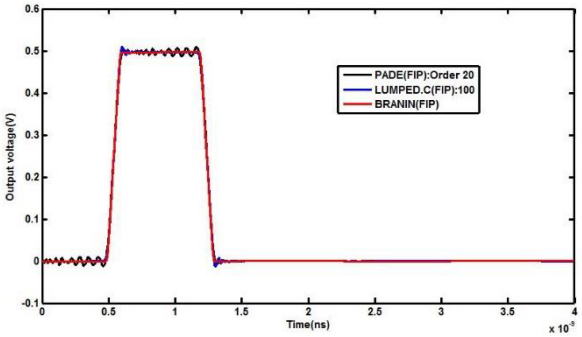

Fig. 7. Transient response of the circuit shown in Fig. 2

Note that in both comparisons, there was excellent agreement between the Pade approximation macro-model on the one hand and the lumped-circuit segmentation macro-model or Branin method on the other.

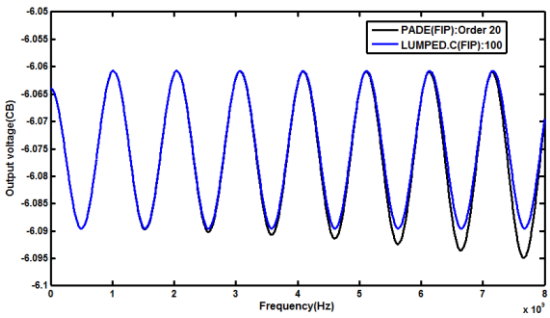

Fig. 8. Frequency response of the circuit shown in Fig.

3.2 Frequency–dependent parameters

Since the dielectric is homogeneous and lossless, only the line's per unit length (p.u.l) inductance and resistance are frequency-dependent. The frequency-dependent parameters of per unit length inductance and resistance are listed in Table 1.

Table 1. Per unit length and resistance parameters of the coupled transmission line

F(GHz)	1e-2	1e-3	1e-2	1e-1	1	3.5	5	10
R(Ω/m)	154	154	154	159	272	432	500	679
L(nH/m)	5.43e+3	5.31e+3	5.32e+3	5.31e+3	5.03e+3	4.90e+3	4.87e+3	4.83e+3

Table 2. Comparison between the lumped-circuit segmentation macro-model and the Pade Approximation

	Padé approximation macro-model	Lumped-circuit segmentation macro-model	Reduction
Number of variables used	109	293	63%

To validate our implementation of Pade approximation, we compared the results from Pade approximation and the traditional, lumped-circuit segmentation macro-model of transmission lines. The line was segmented into 100 segments, each of length $\Delta x = \frac{1}{100}$ cm, to model the frequency-dependent behaviour of the line resistance and inductance. Every segment contained a ladder of order 2.

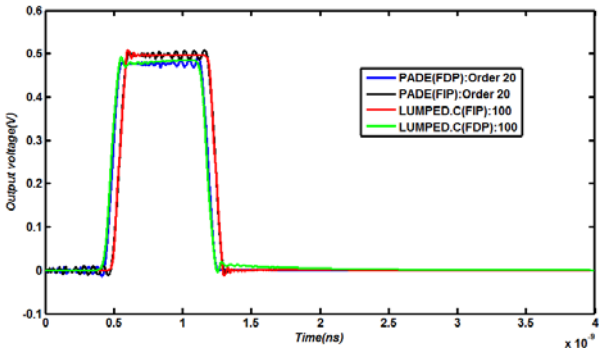

Fig. 9. Transient response of the circuit shown in Fig. 2

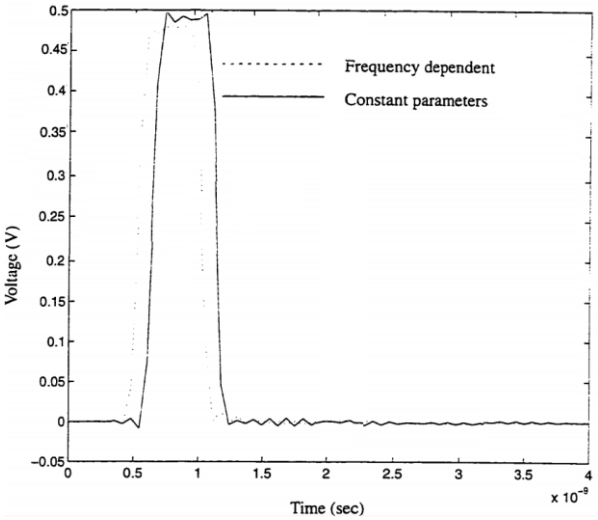

Fig. 10. Transient response of the circuit shown in Fig. 2 from [17]

Figure 9 shows excellent agreement between the Pade approximation and the lumped-circuit segmentation macro-model in the frequency-dependent case. Fig.9 compares the transient response of the transmission line for both the frequency-dependent and the frequency-independent cases. The comparison of the simulation results showed a difference in both amplitude and delay, which is usually related to the skin effect.

Comparing these with the analytical results published by Khazaka [17] shown in Figure 7 shows exact agreement between the results of the hybrid method and analytic method.

In this example, the lumped-segmentation model introduced 293 variables, whereas the proposed method introduced only 109 variables (62% savings), as seen in Table 2.

3.3 Nonlinear terminations

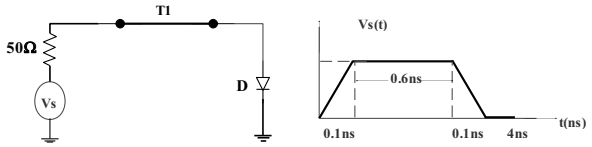

Fig. 11. Electrical representation of the line in Fig. 1 with nonlinear loads.

Figure 11 shows the same transmission structure in Fig.1 but terminated with nonlinear loads. The structure is excited in a similar way to the linear termination case.

Figure 12 shows the transient responses obtained by using two different models; the Pade approximation and the traditional lumped-circuit segmentation macro-model.

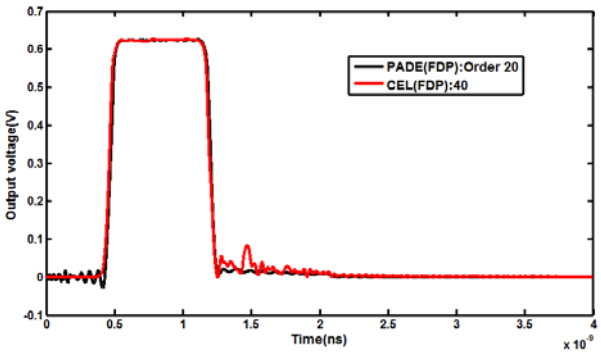

Fig. 12. Transient response of the circuit shown in Fig. 10

The results obtained by our method are in excellent agreement with those obtained by the lumped-circuit segmentation macro-model.

4 Conclusion

In this paper, a new method of modelling transmission lines in the form of a circuit model is presented. This method is based on the theory of transmission lines, as

well as the Pade approximation of the exponential matrix. The method's validity was confirmed by comparing its results with those derived using other methods. It is easy to extend the proposed models to coupled transmission lines with linear and nonlinear terminations. We will discuss this in future papers.

5 References

1. A. Deutch et al., "Modeling and characterization of long on-chip interconnections for high performance microprocessors," IBM J. Res. Develop, 39, pp. 547-567, (1995).
2. A. Deutch et al., "When are transmission-line effects important for on-chip interconnections," IEEE Trans. Microwave 77zeor-yTech., Oct. 1997.
3. A. Semlyen & A. Dabuleanu, "Fast and accurate switching transient calculations on transmission lines with ground return using recursive convolutions," IEEE Transactions on Power Apparatus and Systems, PAS-94(2), pp. 561-571, 1975.
4. J. R. Marti, "Accurate modelling of frequency-dependent transmission lines in electromagnetic transient simulations," IEEE Transactions on Power Apparatus and Systems, PAS-101(1), pp. 147-157, 1982.
5. L. Marti, "Simulation of transients in underground cables with frequency dependent modal transformation matrices," IEEE Transactions on Power Delivery, 3(3), pp. 1099-1110, 1988.
6. Z.. Bouzidi, , A . El Idrissi,.; H .Rouijaa, M .Saih,. Transmission lines modeling approach based on the approximation of Pade. In Proceedings of the 2019 PhotonIcs & Electromagnetics Research Symposium, Rome, Italy, 17–20 June 2019; pp. 4009–4017.
7. C. W. Ho. C. W, "Theory and Computer-aided Analysis of Lossless Transmission Lines, " IBM J. Res. Dev., vol. 17, no. (3), pp. 249-255, May 1973.
8. F. H. Branin, "Transient analysis of lossless transmission lines," Proc. IEEE, 55, (11), pp. 2012-2013, 1967.
9. Y. Mejdoub, H. Rouijaa, && A. Ghammaz, "Transient analysis of lossy multi-conductor transmission lines model based by the characteristics method," Int. J. Eng. Technol., 3 (1), pp. 47–53, (2011).
10. A. Dounavis, X. Li, M. S. Nakhla, & R. Achar, "Passive Closed-Form Transmission-line Model for General-purpose Circuit Simulators," IEEE Trans. Microwave Theory Tech., 47 (12), Dec 1999.
11. Z. Bouzidi, A. El Idrissi, H. Rouijaa, & M. Saih, "Transmission lines modeling approach based on the approximation of Pade," In Proceedings of the 2019 Photonics & Electromagnetics Research Symposium, Rome, Italy, 17–20 June 2019, pp. 4009–4017.
12. C. Yen, Z. Fazarinc, & R. L. Wheeler, "Time-domain skin-effect model for transient analysis of lossy transmission lines," Proc. IEEE, 70, pp. 759-757. July 1982.
13. A. Deutsch, "Electrical characteristics of interconnections for high-performance systems," Proceedings of the IEEE, 86, pp. 315-355, Feb. 1998.
14. J. Vlach & K. Singhal, "Computer Methods for Circuit Analysis and Design". New York: Van Nostrand, 1983.
15. CW. Ho, A. Ruehli, P. Brennan, "The modified nodal approach to network analysis". IEEE Transaction on Circuit and System, vol. 22(No. 6): pp. 504-509, June 1975.
16. R. Khazaka, E. Chiprout, M. Nakhla and Q.J Zhang , "Analysis of high-speed interconnects with frequency dependent parameters" Proc. Int. Symposium on Electromagnetic Compatibility, pp. 203-208, Zurich Switzerland, March 1995.
17. L. INZOLI, H. ROUIJAA “Aseris: Emcap2000-Esacap software” Applications Handbook and Users Manual” DCR /B , janvier 2001